arXiv:cond-mat/0512573v1 [cond-mat.supr-con] 22 Dec 2005

Resonance energy and charge pumping through quantum SINIS contacts

N. B. Kopnin[(1,2)], A. S. Mel'nikov[(3)], and V. M. Vinokur[(4)]
[(1)] *Low Temperature Laboratory, Helsinki University of Technology, P.O. Box 2200, FIN-02015 HUT, Finland,*
[(2)] *L. D. Landau Institute for Theoretical Physics, 117940 Moscow, Russia*
[(3)] *Institute for Physics of Microstructures, 603950, Nizhny Novgorod, GSP-105, Russia*
[(4)] *Argonne National Laboratory, Argonne, Illinois 60439*
(Dated: March 23, 2022)

We propose a mechanism of quantum pumping mediated by the spectral flow in a voltage-biased SINIS quantum junction and realized via the sequential closing of the minigaps in the energy spectrum in resonance with the Josephson frequency. We show that the dc current exhibits giant peaks at rational voltages.

PACS numbers: 73.23.-b, 74.45.+c, 74.78.Na

Quantum pumping in mesoscopic structures offers a unique possibility for studying and direct manipulating the fundamental quantum characteristics of the nanoscale objects (see, for example, [1, 2, 3] and references therein). Most of the previously proposed quantum pumps (including the superconductor–quantum-dot junction of Ref. [4]) used the cyclic adiabatic processes in order to avoid the relaxation which was believed to smear out the quantum behavior [3]. In this Letter we propose and investigate a realization of the *nonequilibrium resonance charge pump* in a form of a superconductor-normal-superconductor (SNS) junction which essentially relies on both the discrete level dynamics due to the adiabatic variation of scattering parameters of the SN contacts and on the relaxation processes in the continuum quasiparticle spectrum. We discuss an exemplary device, the symmetric voltage-biased SINIS structure (see Fig. 1) consisting of two superconducting leads (S) coupled via the (tunnel) barriers (I) and the quantum ballistic normal conductor (N). The dc current (the pumped charge) exhibits giant peaks at rational bias voltages provided the chemical potential of the normal conductor is varied in certain compliance with the Josephson frequency. This requires a nonequilibrium electron distribution achieved under the condition that the Josephson frequency is higher than the inelastic relaxation rate but smaller than the Andreev levels spacing in the normal conductor. The relaxation of this distribution is of critical importance since it enhances the pumping efficiency to the degree that the dc current peaks greatly exceed the rectification current (Shapiro steps) observed in the equilibrium state of the same junction, thus providing unambiguous manifestation of the quantum pumping effect (see the discussion in Ref. [3]).

The normal conductor of the length $d \gtrsim v_x/|\Delta|$ is chosen to have a single conducting mode; here v_x is the Fermi velocity of the conducting mode and $|\Delta|$ is the superconducting gap in the leads. The energy spectrum of sub-gap Andreev states, $\epsilon_n(\phi)$, has a large number $N \sim |\Delta|d/\hbar v_x$ of levels each being a function of the phase difference ϕ between the superconducting leads; a typical spectrum

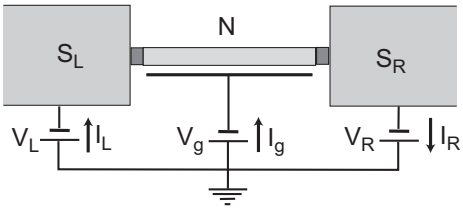


FIG. 1: Charge pump through a quantum channel with a variable chemical potential. The bias voltage is $V = V_L - V_R$.

is shown in Fig. 2(a). For a finite strength Z of barriers between the leads and the normal conductor, the levels are separated by the minigaps $\Delta\epsilon_{2\pi}$ at $\phi = 2\pi k$ and by minigaps $\Delta\epsilon_\pi$ at $\phi = \pi(1+2k)$, where k is an integer [5]. Magnitudes of these minigaps depend on the interference phase $\alpha' = k_x d + \delta$ between the waves incident on and reflected from the barriers (k_x is the Fermi wave vector of the mode and δ is the scattering phase). The minigaps $\Delta\epsilon_\pi$ disappear in the resonance determined by the condition $\sin\alpha' = 0$. In its turn, $\Delta\epsilon_{2\pi}$ disappear in the anti-resonance where $\sin\alpha' = \pm 1$. The Fermi velocity and thus the interference phase α' can be tuned by the gate voltage V_g as shown in Fig. 1. Thus one can close either the gaps at $\phi = 2\pi k$ or the gaps at $\phi = \pi(1+2k)$ sequentially adjusting a proper time dependence of V_g. Choosing the bias voltage $V = (\hbar/2e)d\phi/dt$ such that $\phi = 0$ at the time when the gap $\Delta\epsilon_{2\pi}$ is closed and $\phi = \pi$ at the time when $\Delta\epsilon_\pi$ is closed, and so on, a resonance energy and charge pumping via spectral flow of excitations from states below $-|\Delta|$ to states above $+|\Delta|$ and back will take place realizing an "Archimedean screw" [1] in energy space. The particles moving upwards will reach continuum at $\epsilon = +|\Delta|$ with the distribution corresponding to the equilibrium at $\epsilon = -|\Delta|$ and vice versa. The subsequent relaxation of "wrong" distributions in continuum is accompanied by large dissipation leading to a dc current component under a dc bias voltage. It is essential that the gaps disappeared sequentially: vanishing of just one set of gaps either at $2\pi k$ or at $\pi(1+2k)$ does not lead to the energy or charge pumping. A possible way to

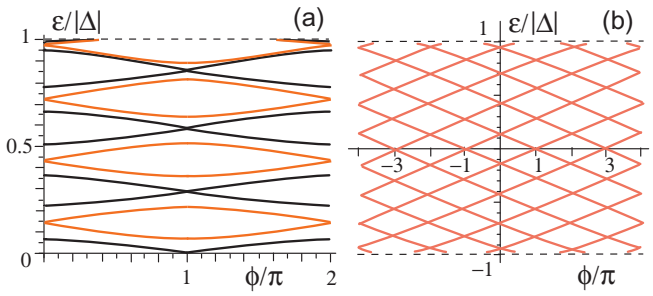


FIG. 2: Energy spectra Eq. (5) for a SINIS contact with $Z = 0.5$ and $\Delta d/\hbar v_x = 10$. (a) Dark lines: In the resonance $\sin\alpha' = 0$; light (red online) lines: in the anti-resonance $|\sin\alpha'| = 1$. (b) Pathes connecting states below $-|\Delta|$ to those above $+|\Delta|$ for trajectories $m = n = 0$ of Fig. 3.

realize this device is to bridge two superconductors by a carbon nanotube [6] subject to a gate voltage. A similar technology was used in Ref. [7] to design semiconductor nanowires with tunable supercurrent.

Resonances.– To close the mini-gaps in resonance with ϕ one needs to tune the amplitude and frequency of the gate voltage in accordance with the bias voltage. Let us plot in Fig. 3 two sets of points in the ϕ, α' plane: (A) points $\phi = 2\pi k$, $\alpha' = \pi(\tilde{k} + 1/2)$ (shown by crosses) and (B) points $\phi = \pi(2k+1)$, $\alpha' = \pi\tilde{k}$ (circles). Resonance is achieved when, changing α' and ϕ with time, one obtains a trajectory that passes first through a point A, then through a point B, then again through A, and so on. For linear trajectories parametrized as $2\alpha' = \omega_g t + 2\pi k$, $\phi - \pi = \omega_J t$, where $\omega_J = 2eV/\hbar$, this requires $\omega_J/\omega_g = (1+2m)/(1+2n)$. Some of these trajectories are shown in Fig. 3 by dashed lines. The resonance trajectories open continuous paths in the ϵ, ϕ space connecting states below $-|\Delta|$ to those above $|\Delta|$, see Fig. 2(b). The gate voltage can be varied within finite intervals along the trajectories [broken lines in Fig. 3] equivalent to the straight lines since $\sin^2\alpha' = \sin^2\omega_g t/2$. More practical is to apply a sinusoidal gate voltage with a frequency Ω. For given m and n, the trajectory passing through the same points is

$$\alpha' \equiv (ed/\hbar v_x)V_g = [(1+2n)\pi/2]\sin(\Omega t) \qquad (1)$$

where $\phi - \pi = \omega_J t$ with $\omega_J = 2\Omega(1+2m)$; the equivalent $\omega_g = 2\Omega(1+2n)$. The amplitude of the gate voltage should be odd rational of $\pi\hbar v_x/2ed$; note that $eV_g \ll \Delta$ for long contacts with $N \gg 1$.

*Spectrum.–*We use the Bogoliubov–deGennes equations

$$\left[-\frac{\hbar^2}{2m}\frac{d^2}{dx^2} - E_F + U(x)\right]\hat{\sigma}_z\hat{\psi} + \hat{H}\hat{\psi} = \epsilon\hat{\psi}\ , \qquad (2)$$

to explicitly demonstrate the resonance properties of the sub-gap energy spectrum of a SINIS structure. Here $\hat{\sigma}_z$ is the Pauli matrix in Nambu space, and

$$\hat{\psi} = \begin{pmatrix} u \\ v \end{pmatrix}\ ,\ \hat{H} = \begin{pmatrix} 0 & \Delta \\ \Delta^* & 0 \end{pmatrix}\ .$$

The superconducting gap is $\Delta = |\Delta|e^{\pm i\phi/2}$ for $x > d/2$ and $x < -d/2$, respectively, while $\Delta = 0$ for $-d/2 < x < d/2$. For simplicity we model the normal reflections at the interfaces as being produced by δ-function barriers $U(x) = I\delta(x - d/2) + I\delta(x + d/2)$.

In the normal region the particle, $e^{\pm iq_+ x}$, and hole, $e^{\mp iq_- x}$, waves have amplitudes $u^\pm$ and $v^\mp$, respectively. The upper or lower signs refer to the waves propagating to the right $\hat{\psi}^> = (u^+, v^-)$ or to the left $\hat{\psi}^< = (u^-, v^+)$. The particle (hole) momentum is $q_\pm = k_x \pm \epsilon/\hbar v_x$. Scattering at the right and left barrier couples the amplitudes of incident and reflected waves [8]:

$$\hat{\psi}_R^< = \hat{S}^R\hat{\psi}_R^>\ ,\ \hat{\psi}_L^> = \hat{S}^L\hat{\psi}_L^<\ ;\ \hat{S} = \begin{pmatrix} S_{11} & S_{12} \\ S_{21} & S_{22} \end{pmatrix}\ . \qquad (3)$$

The scattering matrices for the right and left barriers are $\hat{S}^R = \hat{S}(\chi_2)$ and $\hat{S}^L = \hat{S}(\chi_1)$, respectively, where $\chi_1 = -\phi/2$ while $\chi_2 = \phi/2$. Components of the $\hat{S}$ matrix for δ-like barriers and energies $|\epsilon| < |\Delta|$ are [9]

$$S_{11}(\chi, Z) = S_{22}(\chi, -Z) = -\frac{(U^2 - V^2)(Z^2 + iZ)}{U^2 + (U^2 - V^2)Z^2}\ ,$$
$$S_{12}(\chi, Z)e^{-i\chi} = S_{21}(\chi, Z)e^{i\chi} = \frac{UV}{U^2 + (U^2 - V^2)Z^2}\ .$$

Here $Z = mI/\hbar^2 k_x$ is the barrier strength and $U = 2^{-1/2}[1 + i\sqrt{|\Delta|^2 - \epsilon^2}/\epsilon]^{1/2}$, $V = U^*$. The waves at different ends of the normal channel have different phases

$$\hat{\psi}_R^> = e^{i(\alpha\hat{\sigma}_z + \beta)}\hat{\psi}_L^>\ ,\ \hat{\psi}_R^< = e^{-i(\alpha\hat{\sigma}_z + \beta)}\hat{\psi}_L^< \qquad (4)$$

where $\alpha = k_x d$, $\beta = \epsilon d/\hbar v_x$. Using unitarity of $\hat{S}$ matrix, $\hat{S}^\dagger\hat{S} = 1$, the condition of solvability of Eqs. (3) and (4) assumes a compact form

$$|S_{11}|^2\sin^2\alpha' + |S_{12}|^2\cos^2(\phi/2) = \sin^2(\beta + \gamma)\ . \qquad (5)$$

Here $\alpha' = \alpha + \delta$ and the scattering phase δ is introduced through $\cot\delta = Z$; the phase γ is defined as $e^{2i\gamma} = S_{11}/S_{22}^*$. Equation (5) determines the energy spectrum of a SINIS contact. Such spectrum has been extensively studied by many authors (see e.g. [10]).

In what follows we focus on long contacts, $d \gg \hbar v_x/|\Delta|$, with a large number of levels N. Examples of the spectra are shown in Fig. 2(a). All gaps at $\phi = \pi(1+2k)$ disappear at the same resonance parameter $\sin\alpha' = 0$. Similarly, all gaps at $\phi = 2\pi k$ disappear when $|\sin\alpha'| = 1$. This follows from Eq. (5) due to unitarity $|S_{11}|^2 + |S_{21}|^2 = 1$. The low-energy levels, $\epsilon_n \ll \Delta$, have the form $\epsilon_n = \pm\epsilon_0 + \pi\hbar v_x n/d$ where

$$\epsilon_0 = \frac{\hbar v_x}{d}\arcsin\sqrt{\mathcal{T}^2\cos^2\frac{\phi}{2} + (1 - \mathcal{T}^2)\sin^2\alpha'}\ , \qquad (6)$$

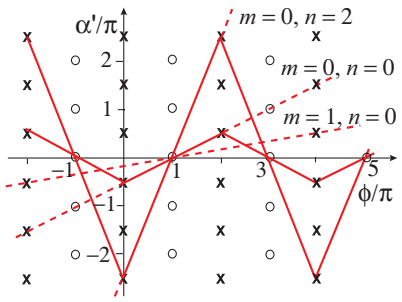


FIG. 3: Linear resonance trajectories.

n is an integer, $\mathcal{T} = (1+2Z^2)^{-1}$, and we use $\gamma \ll 1$. The spectrum has energy gaps at $\phi = \pi(1+2k)$

$$\Delta\epsilon_\pi = (2\hbar v_x/d)\arcsin\left[|\sin\alpha'|\sqrt{1-\mathcal{T}^2}\right] \ .$$

The gaps $\Delta\epsilon_{2\pi}$ at $\phi = 2\pi k$ are given by the same expression with $|\sin\alpha'|$ replaced with $|\cos\alpha'|$. For a transparent contact, $\mathcal{T} = 1$, minigaps disappear.

Current.– For time-dependent E_g and ϕ the current can be calculated [11] by varying Eqs. (2) with respect to $\delta\Delta$ and the chemical potential of the normal conductor controlled by the gate voltage:

$$\delta E_F \equiv \delta E_g(x) = \begin{cases} -e\delta V_g, & |x| < d/2 \\ 0, & |x| > d/2 \end{cases} \ .$$

Note that variations of β, γ, and of the scattering phase δ resulting from changes in k_x are negligible. If the magnitude $|\Delta|$ is constant, $\delta\Delta = i\delta\chi\Delta$, we find

$$(\hbar/2e)\left(\delta\chi_R J_{nR} - \delta\chi_L J_{nL}\right) = \delta\epsilon_n - Q_n\delta V_g \ , \quad (7)$$

where $Q_n = e\int(|u_n|^2 - |v_n|^2)\,dx$ is the charge on level n; the integral in Q_n is extended only over the length of the normal conductor since $|u_n|^2 - |v_n|^2 = 0$ in an open superconducting region. We denote

$$J_n = -(ie\hbar/2m)\left[u_n^*(du_n/dx) + v_n^*(dv_n/dx) - c.c.\right] \ ,$$

$J_{nR,L}$ are the values of J_n near the right (left) barrier.

Let ϵ_n, χ, and E_g adiabatically depend on time as a parameter. Summing up the Andreev states having the distribution function f_n we find the energy balance [11]

$$VI^{sg} = \sum_n (1-2f_n)Q_n\frac{dV_g}{dt} - \sum_n \frac{d\epsilon_n}{dt}(1-2f_n) \ . \quad (8)$$

$I^{sg} = \left(I_R^{sg} + I_L^{sg}\right)/2$ is the current carried by the subgap states, $(\hbar/2)d\chi_{R,L}/dt = -eV_{R,L} = \pm eV/2$ due to symmetry; $V_{R,L}$ and $I_{R,L}^{sg}$ are the potentials and currents in the leads. In Eq. (8), the work done by the bias voltage VI^{sg} and by the gate voltage (the first term in the r.h.s.) produce the energy change of the Andreev states.

Keeping the phases fixed in Eq. (7) we find $Q_n = \partial\epsilon_n/\partial V_g$. Since ϵ_n is a function of two parameters, V_g and ϕ, Eq. (8) contains only the partial derivative

$$I^{sg} = -\frac{2e}{\hbar}\sum_n \frac{\partial\epsilon_n}{\partial\phi}(1-2f_n) \quad (9)$$

where $d\phi/dt = 2eV/\hbar$ was used. This equation formally coincides with the known time-independent result [8, 12].

Note that the average currents satisfy $\overline{I}_g \equiv \overline{I}_R - \overline{I}_L = 0$ where I_g is the gate current (see Fig. 1). Therefore $\overline{I}$ is the average current through each lead. It is determined by the longer time of the particle drift through the levels while the average gate current has also contributions due to much more rapid jumps of the distribution function each time when one of the levels joins the continuum, thus $\overline{I}_g \neq -\sum_n \dot{Q}_n(1-2f_n)$.

Charge pumping.– Consider the simplest case where the gate voltage varies along the broken line in Fig. 3 equivalent to a straight line $m = n = 0$. Let the deviation from the resonances be

$$\phi - \pi = \omega_J t \ , \ 2\alpha' = \omega_J t + 2\alpha_0 \ , \quad (10)$$

where α_0 is determined by initial conditions, and calculate the average current as a function of α_0. As the phase point moves along the trajectory with $\alpha_0 \neq 0$, the distance between nearest levels does not become less than $\Delta\epsilon$. For low energies from Eq. (6) and small α_0,

$$\Delta\epsilon = (\hbar v_x/d)\sqrt{4\mathcal{T}^2(1-\mathcal{T}^2)\alpha_0^2 + \omega_J^2(t-t_0)^2} \ .$$

The probability of Zener tunnelling between the levels is

$$p = \exp\left[-2\pi v_x\mathcal{T}^2(1-\mathcal{T}^2)\alpha_0^2/\omega_J d\right]$$

for all $\phi \approx \pi k$. The Andreev states Eq. (5) are well-defined under an adiabatic condition that p is small far from the avoided crossings, $\omega_J \ll v_x\mathcal{T}^2(1-\mathcal{T}^2)/d$.

Consider first an ideal adiabatic process when transitions between the levels are absent and the distribution f_n on each level is constant. Equation (5) yields

$$\sin[2(\beta+\gamma)]\frac{\partial\beta}{\partial\epsilon}\frac{\partial\epsilon}{\partial\phi} = \frac{1}{2}|S_{12}|^2\sin(\phi-\pi) \ . \quad (11)$$

Note that $\partial\beta/\partial\epsilon = d/\hbar v_x$. The derivatives $\partial\gamma/\partial\epsilon \sim \partial|S|^2/\partial\epsilon \sim (\Delta^2-\epsilon^2)^{-1/2}$ if $Z \sim 1$; they can be neglected for long contacts if ϵ is not very close to Δ. We put $\phi = \phi' + \pi$ in the average $\overline{(\partial\epsilon_n/\partial\phi)} = (2\pi)^{-1}\int_0^{2\pi}(\partial\epsilon_n/\partial\phi)\,d\phi$ and see that $\sin[2(\beta+\gamma)]$ in Eq. (11) does not change its sign, while $\partial\epsilon/\partial\phi$ does if the particle stays on the same level. The average current vanishes for any $\alpha_0 \neq 0$: Pumping is absent without interlevel transitions followed by relaxation of the electronic distribution in continuum.

If p is finite, the particles move up or down the spectrum while the distribution relaxes in continuum due to

fast escape through the potential barriers. The latter requires $\omega_J \ll v_x\mathcal{T}/d$ which is not as strict as the adiabatic condition above. The average current is now finite for nonzero α_0. When p reaches $p=1$ for $\alpha_0=0$, a free drift through the levels is realized along the continuous paths of Fig. 2(b) in the ϵ,ϕ space. The distribution function at each level is again constant though its deviation from equilibrium is the largest: For particles moving down (up) the levels it coincides with the equilibrium $1-2f_n=\pm\tanh(|\Delta|/2T)$ at $\epsilon=\pm|\Delta|$. At this point, the dc current reaches its maximum. For a continuous path Eqs. (5), (11) yield $\beta+\gamma=\pm(\phi-\pi)/2+\pi n$ and

$$\partial\epsilon/\partial\phi=\pm(\hbar v_x/2d)|S_{12}|^2\ . \qquad (12)$$

Transitions from one level to another at the crossing points $\phi=\pi k$ are accompanied by sign changes of $\sin[2(\beta+\gamma)]$ in Eq. (11) while the sign of $\partial\epsilon_n/\partial\phi$ is unchanged; in Eq. (12) it is plus for transitions upwards and minus otherwise. Since the variation in energy for each level is small compared to Δ we finally obtain from Eq. (9) replacing the sum with the integral

$$\begin{aligned}\overline{I}_{max} &= \frac{2ev_x}{d}\tanh\left(\frac{|\Delta|}{2T}\right)\int_{-|\Delta|}^{|\Delta|}|S_{12}(\epsilon)|^2\,\frac{dn}{d\epsilon}\,d\epsilon \\ &= \frac{8e|\Delta|}{\pi\hbar}\frac{\mathcal{T}^2L}{\sqrt{1-\mathcal{T}^2}}\tanh\left(\frac{|\Delta|}{2T}\right)\ , \qquad (13)\end{aligned}$$

where $L=\ln\left[\cot(\delta/2)\right]$. The density of states is $dn/d\epsilon=\pi^{-1}d\beta/d\epsilon=d/\pi\hbar v_x$.

Equation (13) accounts for the dc current from subgap levels (the corresponding superscript is omitted). Continuum states do also contribute. Indeed, for low transparency the Josephson current is [13, 14] $I_J=[ev_x\mathcal{T}^2Y(\alpha')/\pi d]\sin\phi$ where $Y(\alpha')=(2\alpha'-\pi)/\sin(2\alpha'-\pi)$ and $0<\alpha'<\pi$. Dc contributions of the type of Shapiro steps appear when the transparency $\mathcal{T}^2Y(\alpha')$ is ac modulated in resonance with ω_J. However, the magnitude of these steps is proportional to $ev_x\mathcal{T}^2/d$ and is thus much smaller than the dc current in Eq. (13).

Discussion.–It is instructive to look at the energy balance Eq. (8). Since $\phi-\pi=\omega_Jt$, the level sum of separate averages of the second term in the r.h.s. can be written as an integral over one continuous path $\epsilon(\phi)$ (see, Fig. 2(b)). For particles moving upwards, $\sum_n\overline{d\epsilon_n/dt}=(2\pi)^{-1}\int_{\phi_-}^{\phi_+}(d\epsilon/d\phi)\,d\phi$, where $\epsilon(\phi_\pm)=\pm|\Delta|$. Similarly to adiabatic pumps [1, 3] this integral can be viewed as a circulation of a "vector potential" $d\epsilon_n/d\phi$ along a closed contour in the plane of complex Δ (circle of constant $|\Delta|$). Each continuous path provides a nonzero circulation for an adiabatic process that takes place between two dissipative events when the path merges with continuum. This term thus gives a contribution similar to that of multiple Andereev reflection processes in ballistic SNS junctions [15]; in our case the barrier-induced minigaps are closed by the resonance gate voltage. The work by the gate voltage (first term) in Eq. (8) is an energy counterflow; it reduces the pumped charge as compared to its ballistic value. Indeed, $\sum_n\overline{Q_n(dV_g/dt)}=-(\pi\hbar v_x/ed)\sum_n\overline{Q}_n$. The average current is thus proportional to the Andreev probability, $-(\pi\hbar v_x/ed)\sum_n(e+\overline{Q}_n)=-(\pi\hbar v_x/d)\sum_n|S_{12}|^2$ which agrees with Eq. (13).

The energy varies from $-|\Delta|$ to $+|\Delta|$ during time $T_0\sim|\Delta|d/\hbar v_F\omega_J$ which should be shorter than the inelastic relaxation time τ_ϵ. Combined with the adiabatic condition this gives the Josephson frequency window for the first resonance, $|\Delta|d/\hbar v_F\tau_\epsilon\ll 2eV/\hbar\ll v_F\mathcal{T}^2(1-\mathcal{T}^2)/d$. Such slow τ_ϵ^{-1} requires the use of low temperatures.

In the case of a sinusoidal gate voltage Eq. (1), resonances also occur for rational gate voltage amplitudes specified by n and for $\omega_J=2\Omega(1+2m)$. The dc current-voltage curve has peaks $\bar{I}_m\sim\bar{I}_{max}/(1+2m)$ decaying with m but weakly depending on n. The frequency $2eV/\hbar(1+2m)$ should also belong to the window above. This puts an upper limit on observation of peaks of higher order in m. Ideally, the largest peak $\overline{I}_{max}$ is N times higher than the usual Shapiro step.

To summarize, we found a new mechanism of nonequilibrium charge pumping. It is based on the spectral flow in a voltage-biased SINIS quantum junction when the minigaps in the energy spectrum are closed sequentially in resonance with the Josephson frequency.

We thank Yu. Galperin and V. Kozub for valuable discussions. This work was supported, in part, by the US DOE Office of Science, contract No. W-31-109-ENG-38, by Russian Foundation for Basic Research, by Russian Science Support Foundation, and by Program "Quantum Macrophysics" of RAS. ASM acknowledges the support by the Academy of Finland.

[1] B.L. Altshuler, L.I. Glazman, Science **283**, 1864 (1999).
[2] M. Switkes, C.M. Marcus, K. Campman, A.C. Gossard, Science **283**, 1905 (1999).
[3] M. Moskalets and M. Büttiker, Phys. Rev. B **72**, 035324 (2005); M. Büttiker, J. Low Temp. Phys. **118**, 519 (2000).
[4] M. Governale, F. Taddei, R. Fazio, and F.W.J. Hekking, cond-mat/0506078.
[5] P. F. Bagwell, Phys. Rev. B **46**, 12573 (1992).
[6] M.R. Buitelaar, W. Belzig, T. Nussbaumer, et al., Phys. Rev. Lett. **91**, 057005 (2003); A. Kosumov, M. Kociak, M. Ferrier, et al., Phys. Rev. B **68**, 214521 (2003).
[7] Y.J. Doh, J.A. van Dam , A.L. Roest, et al., Science **309**, 272 (2005).
[8] C.W.J. Beenakker, Phys. Rev. Lett. **67**, 3836, (1991).
[9] G.E. Blonder, M. Tinkham, and T.M. Klapwijk, Phys. Rev. B, **25**, 4515 (1982).
[10] U. Schüssler and R. Kümmel, Phys. Rev. B **47**, 2754 (1993); G.A. Gogadze and A.M. Kosevich, Fiz. Nizkih Temp. **24**, 716 (1998) [Low Temp. Phys. **24**, 540 (1998)]; A. Jacobs and R. Kümmel, Phys. Rev. B **71**, 184504 (2005); D.D. Kuhn, N.M. Chtchelkatchev, G.B. Lesovik, and G. Blatter, Phys. Rev. B, **63**, 054520 (2001).

[11] N.I. Lundin, L.Y. Gorelik, R.I. Shekhter, M. Jonson, Superlattices and Microstructures, **25**, 937 (1999).
[12] A.A. Golubov, M.Yu. Kupriyanov and E. Il'ichev, Rev. Mod. Phys. **76**, 411 (2004).
[13] A. Furusaki, H. Takayanagi, and M. Tsukada, Phys. Rev. B **45**, 10563 (1992).
[14] A.V. Galaktionov and A.D. Zaikin, Phys. Rev. B **65**, 184507 (2002).
[15] U. Gunsenheimer and A.D. Zaikin, Phys. Rev. B **50**, 6317 (1994).